The B2-B19-B19′ transformation in a rapidly solidified Ti-45Ni-5Cu(at%) alloy

TAE-HYUN NAM, JAE-HWA LEE, KI-WON KIM, HYO-JUN AHN
Division of Materials Engineering and ERI, Gyeongsang National University, 900 Gazwa-dong, Chinju, Gyeongnam 660–701, Korea

YEON-WOOK KIM
Department of Material Engineering, Keimyung University, 1000 Shindang-dong, Dalseo-gu, Taegu 704-710, Korea

Rapidly solidified Ti-Ni alloys have been known to show transformation behavior different from that of alloys fabricated by conventional ingot making. Ti-Ni alloy ribbons fabricated by melt spinning transformed in two-stage, i.e., the B2-R-B19′, while alloys fabricated by ingot making transformed in one-stage, i.e., the B2-B19′[1, 2]. The change in transformation behavior by melt spinning was attributed to an introduction of high density of dislocations and the formation of very fine coherent Ti_2Ni particles which resulted in a strong resistance to the lattice deformation associated with a formation of the B19′ martensite [1, 2].

Fully annealed Ti-Ni-Cu alloys whose Cu-content is less than 5 at% showed the one-stage B2-B19′ transformation [3]. On increasing Cu-content up to 7.5 at%, the B2-B19′ transformation was suppressed and the B19 martensite appeared, and consequently the alloys showed the two-stage B2-B19-B19′ transformation [4]. If the introduction of dislocations and the formation of Ti_2Ni particles accompanied with rapid solidification suppressed the B2-B19′ transformation in Ti-Ni-Cu alloys, the two-stage B2-B19-B19′ transformation was expected to occur even in the ribbon alloys with Cu-content less than 7.5 at%. The purpose of the present study is, therefore, to investigate transformation behavior of a rapidly solidified Ti-45Ni-5Cu alloy and to correlate the transformation behavior with microstructural changes by rapid solidification. An effect of melt temperatures on transformation behavior of ribbons will also be discussed. Ribbons for the present study were prepared by melt spinning from a pre-alloy with the composition of Ti-45Ni-5Cu(at%). The melt temperature was varied from 1673 to 1873 K for examining its effect on transformation behavior of the ribbons. Linear velocity was 31 m/s. Transformation behavior of the ribbons was investigated by differential scanning calorimetry (DSC) and X-ray diffraction (XRD). Microstructure of the ribbons was investigated using a transmission electron microscope (TEM) operated at 200 kV.

Fig. 1 shows XRD patterns of as-spun Ti-45Ni-5Cu ribbons fabricated at various melt temperatures. All patterns were obtained from the free sides of ribbons. In the pattern obtained from the ribbons fabricated at melt temperature of 1673 K, as can be seen in Fig. 1a, diffraction peaks associated with the B19′ martensite appear. In the patterns obtained from the ribbons with melt temperatures of 1773 and 1873 K, as seen in Fig. 1b and c, diffraction peaks of the B2 parent phase appear. Therefore, it is nown that as-spun Ti-45Ni-5Cu alloy ribbons are crystalline. Fig. 2 shows DSC curves of Ti-45Ni-5Cu alloy ribbons. In the curve of ribbons fabricated at melt temperature of 1673 K, as can be seen in Fig. 2a, one exothermic peak and one endothermic peak appear on cooling and heating curves, respectively. However, in the curves of ribbons with melt temperatures of 1773 and 1873 K, as seen in Fig. 2b and c, two exothermic peaks and two endothermic peaks appear on cooling and heating curves, respectively.

In rapidly solidified Ti-25Ni-25Cu alloy ribbons, a split on DSC peaks was observed and ascribed to the difference in microstructures between free side and wheel side of ribbons [5]. In Ti-45Ni-5Cu ribbons, however, the split on DSC curves in Fig. 2b and c is not attributed to the difference in microstructures between free side and wheel side of ribbons because it was observed even after removing wheel side by mechanical grinding followed by electropolishing [6].

In order to explain DSC peaks in Fig. 2, XRDs were made as specimens cooled. Fig. 3 shows XRD patterns of the ribbons fabricated at melt temperature of 1673 K. On cooling the specimen, at 323 K, the diffraction peaks of the B19′ martensite start to appear. On further cooling, at 303 K, intensity of a diffraction peak of the B2 parent phase decreases, while those of the B19′ martensite increase. On further cooling, at 289 K, the diffraction peak of the B2 parent phase disappears and only the diffraction peaks of the B19′ martensite are found. Therefore, the DSC peaks in the curve of Fig. 2a are ascribed to the B2-B19' transformation. Fig. 4 shows XRD patterns of the ribbons fabricated at melt temperature of 1873 K. At 323 K, only the diffraction peaks of the B2 parent phase are seen. On cooling, at 253 K, the diffraction peaks of the B19 martensite start to appear. On further cooling, at 233 K, the diffraction peaks of the B19′ martensite start to appear. On further cooling, at 143 K, intensity of the diffraction peaks of the B19′ martensite increases. Therefore, the DSC peak on cooing designated by Ms′* in the curve of Fig. 2c is attributed to the B2–B19 transformation and that designated by Ms* is ascribed to the B19-B19′ transformation. From Figs 3 and 4, it is concluded that

0022-2461 © *2005 Springer Science + Business Media, Inc.*

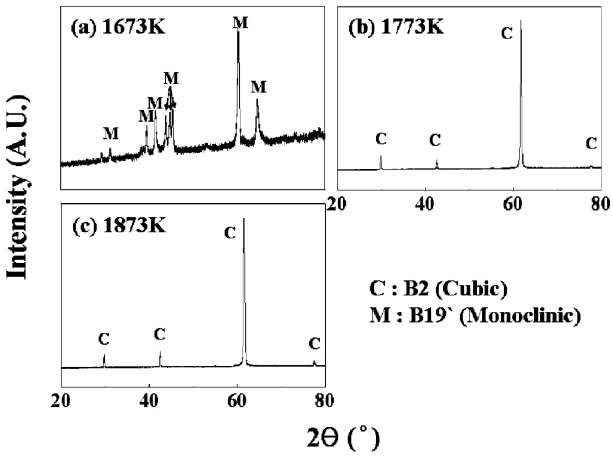

Figure 1 XRD patterns obtained from the free side of Ti-45Ni-5Cu alloy ribbons fabricated at various melt temperatures.

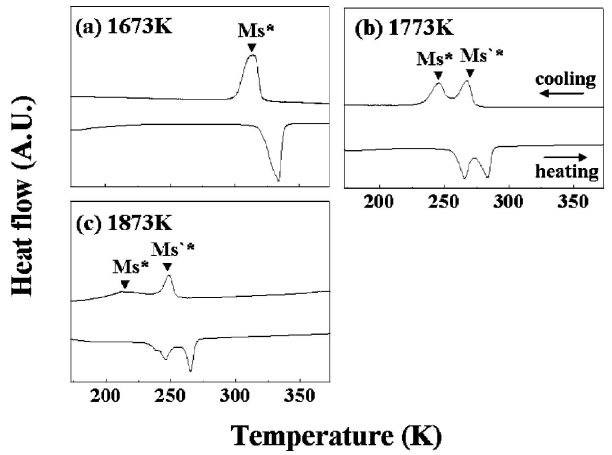

Figure 2 DSC curves of Ti-45Ni-5Cu alloy ribbons fabricated at various melt temperatures.

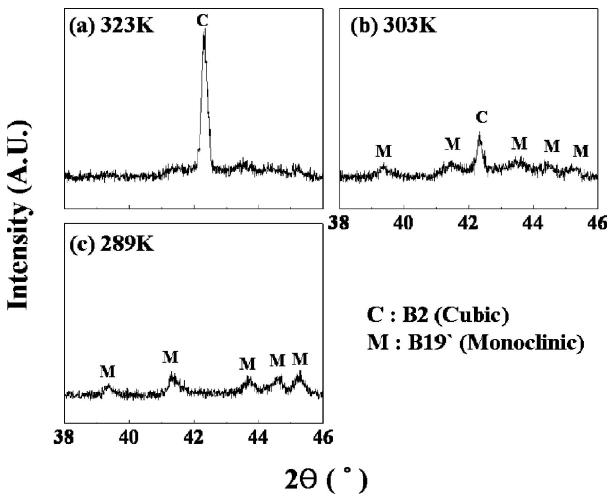

Figure 3 XRD patterns of Ti-45Ni-5Cu alloy ribbons fabricated at 1673 K melt temperature during cooling.

transformation behavior of rapidly solidified Ti-45Ni-5Cu ribbons depends on melt temperature. The one-stage B2-B19′ transformation occurs in the ribbons fabricated at the melt temperature below 1673 K, while the two-stage B2-B19-B19′ transformation occurs in those fabricated at the melt temperatures above 1773 K.

In order to clarify the reason for the change in transformation behavior depending on melt temperature, microstructures of the ribbons were examined by TEM observations. Fig. 5a is a bright field image of the ribbon fabricated at the melt temperature of 1673 K and Fig. 5d is an electron diffraction (ED) pattern corresponding to a, which is explained by the B19′ martensite. Fig. 5b is a bright field image of the ribbon fabricated at the melt temperature of 1773 K. Very fine spherical particles with radius about 14 nm are found. Those particles are known to be Ti_2Ni phase with coherency with the B2 parent phase matrix from e. In Fig. 5a, however, they are not found. As mentioned before, the two-stage B2-B19-B19′ transformation behavior was observed in the ribbons fabricated at the melt temperature of 1773 K, while the one-stage B2-B19′ transformation behavior was seen in those fabricated at the melt temperature of 1673 K. This suggests that the coherent Ti_2Ni particles play an important role inducing the B19 martensite.

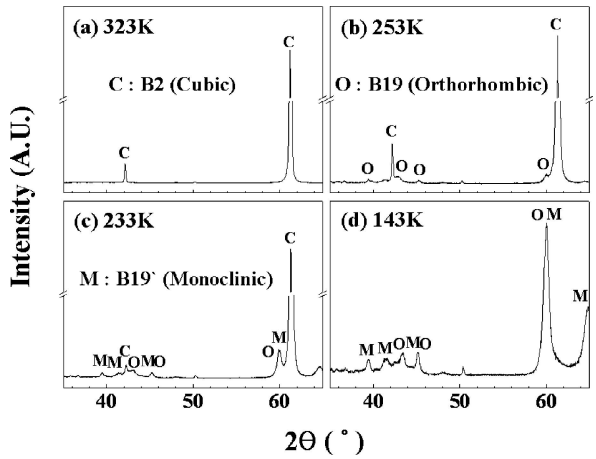

Figure 4 XRD patterns of Ti-45Ni-5Cu alloy ribbons fabricated at 1873 K melt temperature during cooling.

Fig. 5c is a bright field image of the ribbon fabricated at the melt temperature of 1873 K. Similar to Fig. 5b, very fine spherical particles with radius about 12 nm are found. Those particles are also known to be Ti_2Ni phase with coherency with the B2 parent phase matrix from f. Comparing Fig. 5b and c, it is found that volume fraction of coherent Ti_2Ni particles increases from 10 to 40% with raising melt temperature, although a change in size of the particles is very small. The increase in volume fraction of Ti_2Ni particles is possibly ascribed to the increase in cooling rate by raising melt temperature [6, 7]. Since the coherent Ti_2Ni particles play an important role in inducing the B19 martensite, it is expected that the stability of the B19 martensite increases with raising of the melt temperature. As stability of the B19 martensite increases, a temperature gap between Ms′* and Ms* is expected to increase. Fig. 6 shows a relationship between the temperature gaps and melt temperature. It is found that the temperature gap increases with rising melt temperature.

In melt-spun binary Ti-Ni alloy ribbons, similar coherent Ti_2Ni particles were observed. In the ribbons, the particles induced the R phase, and consequently the two-stage B2-R-B19’ transformation occurred. In contrast to the binary alloy ribbons, coherent Ti_2Ni particles in Ti-45Ni-5Cu alloy ribbons did not induce the R phase, but induced the B19 martensite. This

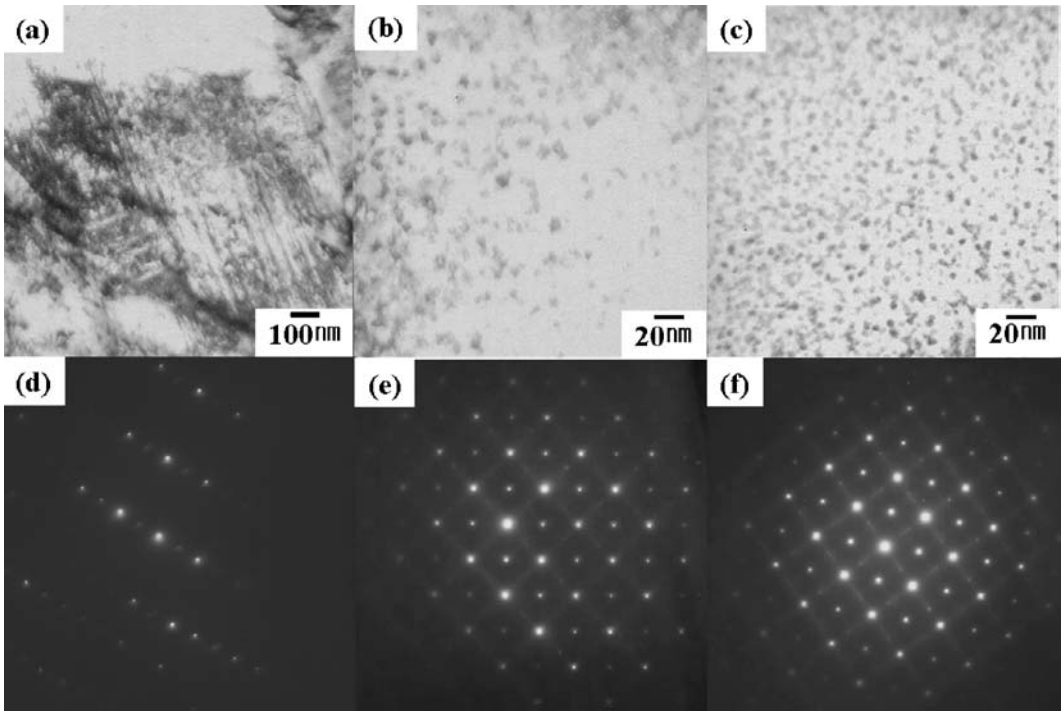

Figure 5 TEM observation results of the Ti-45Ni-5Cu alloy ribbons. (a), (b) and (c) are bright field images of ribbons fabricated at melt temperatures of 1673, 1773 and 1873 K, respectively. (d), (e) and (f) are electron diffraction patterns corresponding to (a), (b) and (c), respectively.

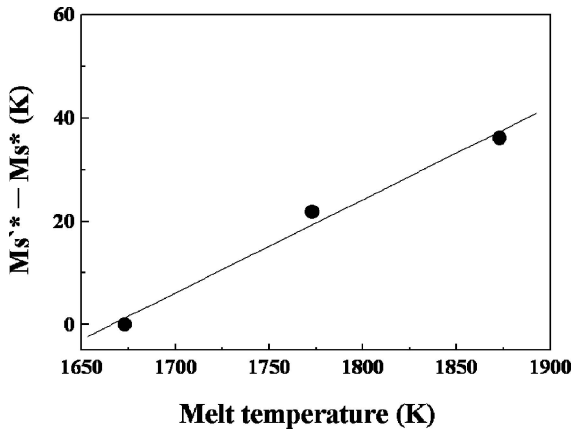

Figure 6 Relationship between $Ms'^{*} - Ms^{*}$ and melt temperature in Ti-45Ni-5Cu alloy ribbons.

difference is ascribed to Cu which increases a stability of the B19 martensite [8].

Melt-spun Ti-45Ni-5Cu(at%) alloy ribbons transformed in two-stage, i.e., the B2-B19-B19' when melt temperature was higher than 1773 K, while they transformed in one-stage, i.e., the B2-B19′. The two-stage transformation behavior was attributed to Ti_2Ni particles (≈12 nm) with coherency with matrix which made a strong resistance to lattice deformation associated with a formation of the B19′ martensite. A stability of the B19 martensite increased with raising melt temperature.

Acknowledgements

This research was supported by University IT Research Center Project

References

1. T. H. NAM, J. P. NOH, D. W. JUNG, Y. W. KIM, H. J. IM, J. S. AHN and T. MITANI, *J. Mat. Sci. Lett.* **21** (2002) 685.
2. T. H. NAM, J. H. KIM, M. S. CHOI, Y. W. KIM, H. J. IM, J. S. AHN and T. MITANI, *ibid.* **21** (2002) 799.
3. Y. SHUGO, F. HASEGAWA and T. HONMA, *Bull. Res. Inst. Mineral Dress. Metall.* **37** (1981) 80.
4. T. H. NAM, T. SABURI and K. SHIMIZU, *Mater. Trans* .JIM **31** (1990) 956.
5. H. RÖSNER, A. V. SHELYAKOV, A. M. GLEZER and P. SCHLOβMACHER, *Mater. Sci. Eng.* **A273–275** (1999) 733.
6. T. H. NAM, J. H. LEE, T. Y. KIM and Y. W. KIM, *Mat. Sci. Forum.* **449–452** (2004) 1093.
7. R. NAGARAJAN and K. CHATTOPADHYAY, *Acta Metall. Mater.* **42** (1994) 947.
8. T. FUKUDA, T. KAKESHITA, H. HOUJOU, S. SHIRAISHI and T. SABURI, *Mater. Sci. and Engr.* **A273–275** (1999) 166.

Received 30 June 2004
and accepted 20 January 2005